MIT Open Access Articles

On the Role of Heterogeneous Chemistry in Ozone Depletion and Recovery

Wilka Catherine (Orcid ID: 0000-0002-2917-1140)
Stone Kane, A. (Orcid ID: 0000-0002-2721-8785)
Solomon Susan (Orcid ID: 0000-0002-2020-7581)
Mills Michael, James (Orcid ID: 0000-0002-8054-1346)
Schmidt Anja (Orcid ID: 0000-0001-8759-2843)

On the role of heterogeneous chemistry in ozone depletion and recovery

Catherine Wilka[1], Kasturi Shah[1], Kane Stone[1], Susan Solomon[1], Douglas Kinnison[2], Michael Mills[2], Anja Schmidt[3,4], and Ryan R. Neely III[5,6]

[1] Department of Earth, Atmospheric, and Planetary Sciences, Massachusetts Institute of Technology, Cambridge, MA 02139

[2] Atmospheric Chemistry Observations and Modeling Laboratory, National Center for Atmospheric Research, Boulder, CO 80307

[3] Department of Chemistry, University of Cambridge, Lensfield Road, Cambridge CB2 1EW, UK

[4] Department of Geography, University of Cambridge, Downing Place, Cambridge CB2 3EN, UK

[5] School of Earth and Environment, University of Leeds, Leeds, UK

[6] National Centre for Atmospheric Science, University of Leeds, Leeds, UK.

Corresponding author: Catherine Wilka (cwilka@mit.edu)

Key Points:

- Heterogeneous chemical reactions on volcanic sulfate aerosols from Mt. Pinatubo and El Chichón deepened ozone depletion from 1979-1998

- Heterogeneous reactions have delayed ozone recovery from 1999-2014, mainly due to a series of moderate eruptions after 2004

- Accurate representation of heterogeneous chemistry is essential when detecting ozone recovery trends

Abstract

We demonstrate that identification of stratospheric ozone changes attributable to ozone depleting substances and actions taken under the Montreal Protocol requires evaluation of confounding influences from volcanic eruptions. Using a state-of-the-art chemistry-climate model, we show that increased stratospheric aerosol loading from volcanic eruptions after 2004 impeded the rate of ozone recovery post-2000. In contrast, eruptions increased ozone loss rates over the depletion era from 1980 to 1998. We also present calculations without any aerosol chemistry to isolate contributions from gas-phase chemistry alone. This study reinforces the need for accurate information regarding stratospheric aerosol loading when modeling ozone changes, particularly for the challenging task of accurately identifying the early signs of ozone healing distinct from other sources of variability.

Plain Language Summary

This study examines the impact of volcanic eruptions on ozone depletion and recovery. Volcanic eruptions increase stratospheric aerosols and thereby enhance ozone depletion. Model simulations indicate that several large eruptions increased the rate of ozone depletion from 1979-1998, while a series of moderate eruptions after 2004 slowed the rate of ozone recovery from 1999-2014. The Montreal Protocol's effectiveness in restoring the ozone layer can be expected to emerge most clearly whenever volcanically quiescent periods occur in the future.

1 Introduction

The potential of anthropogenic chlorofluorocarbons (CFCs) to deplete ozone via gas-phase photochemistry was recognized in the 1970s (Molina & Rowland, 1974). This chemistry was expected to cause a small decrease in total ozone by 2100 if CFC production continued. The urgency of the problem increased dramatically when Antarctic observations showed a sharp, unexpected ozone decline in the 1980s (Farman et al., 1985). Referred to as the ozone "hole," this dramatic thinning of the ozone layer is the result of heterogeneous reactions on cold polar stratospheric cloud surfaces that activate chlorine from the reservoir species $ClONO_2$ and HCl to form reactive species capable of catalytic ozone destruction (Solomon et al., 1986). Laboratory studies along with observations of ozone losses following the 1982 El Chichón volcanic eruption prompted examination of heterogeneous processes on liquid sulfuric acid/water aerosols, including the hydrolysis of N_2O_5; this reaction was found to

display little temperature sensitivity and to be of importance for the smaller ozone losses occurring in the global lower stratosphere (Hofmann & Solomon, 1989; Rodriguez et al., 1991). Measurements not only of ozone but also of other species including NO and ClO following the 1991 eruptions of Mt. Pinatubo and Cerro Hudson confirmed that the stratospheric sulfuric acid aerosol enhancements from volcanic eruptions can perturb atmospheric composition even under warm conditions at midlatitudes via N_2O_5 hydrolysis (Solomon, 1999 and references therein). Recently it has been suggested that stratospheric sulfate aerosols can also cause chlorine activation in the tropics, with recent eruptions such as Nabro in 2011 enhancing this effect (Solomon et al., 2016a). Trends are expected to vary based on future stratospheric aerosol burdens in the 21st century (Naik et al., 2017; Klobas et al., 2017).

Concerns about ozone depletion led the world to adopt the Montreal Protocol to phase out ozone depleting substances (ODS), and observations do show a decline in HCl from the peak values around the year 2000 (Mahieu et al., 2014; Rinsland et al., 2003), in good agreement with the model used here (Douglass et al., 2014). In accordance with models, observations suggest ozone recovery is emerging (Chehade et al., 2014; Sofieva et al., 2017; Solomon et al., 2016b), although the significance of trends depends strongly on the magnitude of the background atmospheric variability (Keeble et al., 2018), and varies with latitude and season.

In this paper, we use observations of volcanic sulfur loading together with model calculations to analyze how heterogeneous chemistry has affected ozone trends in both the depletion and recovery eras. The contribution of gas-phase chemistry alone has not been often revisited since the discovery of heterogeneous chemistry in the 1980s, and here we also evaluate gas-phase depletion with a state of the art chemistry-climate model.

2 Materials and Methods

2.1 Model Description

To examine ozone trends in runs with different forcings we use the Whole Atmosphere Community Climate Model, version 4 (WACCM4). WACCM is a component of the Community Earth System Model, version 1 (CESM1) from NCAR. It is a high-top model with fully interactive gas-phase and heterogeneous chemistry that has been evaluated via multiple comparisons with data and other models (Garcia et al., 2017; Marsh et al., 2013; Solomon et al., 2015; Wegner et al., 2013). It has a spatial resolution of 1.9° by 2.5° latitude-longitude grid with 88 pressure levels up to 140 km. We use the specified dynamics mode (SD-WACCM) in which the model below 50 km is nudged to temperature, wind, and surface pressure fields from NASA's Modern-Era Retrospective Analysis for Research and Applications (MERRA) with a relaxation time of 50 hours.

The aerosol microphysics scheme was updated and the volcanic sulfur emissions are taken from a database of eruptions developed by Neely and Schmidt (2016), implemented in a modal aerosol model which compares favorably to available observations for both high and low aerosol loadings (Mills et al., 2016).

We present results that incorporate different forcings to test the relative impacts of (i) our best representation of both background and volcanic aerosols since 1979 (Chem-Dyn-Vol, modal aerosol model), (ii) background aerosols under volcanically clean conditions (Vol-Clean), (iii) omission of low latitude heterogeneous chlorine chemistry (NoHet40NS), and (iv) gas-phase chemistry only. We include volcanic aerosols but turn off all heterogeneous chlorine chemistry between 40°N and 40°S in the run labeled "NoHet40NS"; N_2O_5 hydrolysis is, however, included in this case. Every run includes historical anthropogenic emissions of ozone depleting substances and greenhouse gases, and is spun up using a repeating series of the 1979-1982 meteorological fields beginning in 1952 before being nudged to MERRA dynamics beginning in 1979, when the MERRA reanalysis starts; the calculations extend to 2014, based upon availability of consistent MERRA and solar flux input datasets that drive the model.

2.2 SBUV and NIWA-BS Total Column Ozone

We compare the total column ozone (TCO) trends simulated by WACCM against observational data from both the Solar Backscatter Ultraviolet (SBUV) MOD v8.6 and the National Institute of Water and Atmospheric Research - Bodeker Scientific (NIWA-BS) data sets for the depletion era of 1979-1998 and the recovery era of 1999-2014. The SBUV data set is derived from multiple backscatter instruments and the TCO product agrees with ground-based ozone measurements to better than 1% after 1978 (McPeters et al., 2013). NIWA-BS is a merged data set which incorporates multiple satellite-based measurements, including SBUV, corrected for biases and drifts through comparisons with ground-based spectrophotometer networks (Bodecker et al., 2005).

2.3 SWOOSH Vertical Ozone

To examine vertically resolved trends we use the 2.5° resolution combined product from the Stratospheric Water and OzOne Homogenized (SWOOSH) data set (Davis et al., 2016). The SWOOSH data begins in 1984, so for all vertically resolved trend analysis we use the period 1984-1998 to represent what we refer to as the SWOOSH depletion era, with the recovery era defined as before. We present the SWOOSH data only as a general point of comparison, recognizing that there are substantial differences in trends among different data sets and the quantification of satellite ozone trends across different datasets is a topic of current research (see, e.g., Steinbrecht et al., 2017).

3 Global Trends

We first examine trends in total ozone for both the depletion and recovery eras. The top panel of Figure 1 shows model and data time series anomalies over the entire run, and for the depletion and recovery eras in the lower left and right panels, respectively. Figure S1 shows the same for absolute total column ozone. The comparison of the gas-phase only run to the other cases illustrates the impact of heterogeneous chemistry (note that all runs use the same prescribed MERRA dynamics); however, any dynamical trends along with gas phase chemistry will influence all the runs, see below. We use a 3-year running mean to smooth the QBO and other high frequency variability, then take an average from 60°N to 60°S and zero each time series to its 1998 value before fitting the anomalies in the depletion era and the recovery era separately with a linear least squares model. Volcanic eruptions are indicated by triangles at the bottom of the panels, with the larger triangles indicating eruptions of magnitude 5 and 6 on the Volcanic Explosivity Index (VEI) scale. Chem-Dyn-Vol shows distinct departures from Vol-Clean during times of increased volcanic aerosol loading. The influence of volcanic eruptions on these long term (10-20 year) ozone trends depends on their magnitudes and timing. The calculated depletion from Mt. Pinatubo and Cerro Hudson lingers into the mid-1990s and those enhanced ozone losses (Chem-Dyn-Vol versus Vol-Clean in Figure 1) towards the end of the depletion

era imply steeper depletion over that period. In the recovery era, very low stratospheric aerosol loads characterize the start of the period near 1999, followed by several moderate eruptions after about 2005 (Solomon et al., 2011; Vernier et al., 2011), implying ozone losses in Chem-Dyn-Vol compared to Vol-Clean that flatten trends in the recovery era. The slopes and 95% confidence intervals for linear fits are given in Table 1 in Dobson Units (DU) per year, along with the percentage differences of each trend from Chem-Dyn-Vol. Tables S1 and S2 show the same for the Northern and Southern Hemispheres. Table S3 lists eruptions that transported SO_2 amounts greater than 0.03 Tg to 10 km or higher.

Figure 1 and Table 1 show that the evolution of the total column ozone has been strongly dominated by heterogeneous chemistry. Vol-Clean trends are about 16% less negative than Chem-Dyn-Vol in the depletion era and 52% more positive in the recovery era (Table 1), showing how volcanoes have increased the ozone loss in the depletion era and delayed the recovery according to this model. NoHet40NS trends are about 5% less negative than Chem-Dyn Vol in the depletion era and 12% more positive in the recovery era, showing how heterogeneous chemistry in the tropics and subtropics has also contributed to global trends. Chem-Dyn-Vol, Vol-Clean, and NoHet40NS trends in the depletion era show less depletion but greater variability in the Northern Hemisphere, while in the recovery era these trends show stronger recovery but greater variability in the Southern Hemisphere.

Some ozone trend studies using both observations (Chehade et al., 2014; Weber et al., 2018) and models (Keeble et al., 2018) employ multiple linear regression (MLR) deal with contributions including the 11-year solar cycle, ENSO, the QBO, and volcanic influences. While linear regression can reduce error bars (for example, by accounting for QBO variability), it generally does not change the magnitude or structure of absolute trends (e.g., Ball et al. 2018). Figure S2 shows SWOOSH trends for the recovery era using a multiple regression including a representation of solar, QBO, ENSO, and aerosol terms (described further in Text S2; see also Stone et al., 2018), and the differences between Figures S2 and 3 (linear regression) are minimal. We note that time lags and relationships between volcanoes and ozone vary in latitude and altitude, impeding identification of a simple regression index such as integrated aerosol columns. Further, it is clear that volcanic aerosols are especially effective for ozone loss under cold conditions, and such temperature-aerosol coupling is not accounted for in simple linear regressions. While it may be possible to formulate a non-linear and/or mixed-term regression model that fully accounts for aerosol impacts, in this paper our goal is to assess how aerosols have impacted the raw data, so we have chosen to perform simple linear trends rather than a multiple regression. In addition, quantifying the calculated influence of volcanic aerosols on ozone trends is important for its own sake, and can inform studies seeking to account for it using multiple regression methods.

Comparison of the model to the SBUV and NIWA-BS total column time series shows good general agreement. The two observational data sets track each other closely in anomaly space in the depletion era, although Figure S1 shows that NIWA-BS is lower overall, except in the years immediately after Pinatubo. The discrepancy between them may be due to NIWA-BS's prioritization of other instruments over SBUV. Both data series display somewhat less depletion from Pinatubo/Hudson than Chem-Dyn-Vol in the early 1990s, but more than Vol-Clean or the gas-phase run. Note that the gas-phase run best shows the variations associated with the solar cycle, whose effect maximizes in the upper stratosphere. Trend lines show that the gas-phase only run fails to capture the trend in the depletion era. While the Chem-Dyn-Vol and Vol-Clean results are closer to the observations, their depletion era trends are somewhat steeper than the data (although only Chem-Dyn-Vol is different at the 95% confidence level).

In the recovery era, both observational datasets suggest trends that display less recovery (positive trends) than the Chem-Dyn-Vol or Vol-Clean means, although Chem-Dyn-Vol is closer to the observations and all overlap at the 95% confidence interval as given in Table 1. The NIWA-BS dataset shows a deeper negative anomaly in the mid-2000s than the model, and is again lower overall in Figure S1, whereas the SBUV data track Chem-Dyn-Vol closely there. In contrast, both the NIWA-BS and Chem-Dyn-Vol show an uptick of similar magnitude after 2012, whereas the SBUV data stays mostly flat for the last few years.

4 Trends in Latitude and Height

Figures 2 and 3 show contour plots of linear trends during the SWOOSH depletion (1984-1998) and recovery (1999-2014) eras, respectively. Each figure shows the annual average linear trends for the Chem-Dyn-Vol, Vol-Clean, and gas-phase model runs and the SWOOSH data set. For each panel, the time series has had high frequency variability removed before trend calculation by applying a 3-year running mean, as in Figure 1. Our results are similar to those over nearly the same years based on SAGE II and GOMOS data (Kyrölä et al., 2013, their Figures 13 and 14). Trends are fitted separately at each latitude-pressure point and then expressed as percent per decade relative to the mean of the ozone mixing ratio for each era. Figures S3 and S4 show the differences between the Chem-Dyn-Vol run and the three other runs (Vol-Clean, Gas-phase, and NoHet40NS) for the selected depletion and recovery eras, respectively.

Gas-phase chemistry is expected to dominate upper stratospheric changes, and Figure 2 shows that observed depletion for pressures lower than 20 hPa broadly agrees with the gas-phase only run (the other simulations are similar since there is no significant heterogeneous chemistry in the upper stratosphere). Turning to the lower stratosphere in Figure 2, the greatest depletion occurs in the high latitude lower

stratospheres of both hemispheres where PSCs can form, with the Antarctic showing deeper depletion than the Arctic due to its lower temperatures and more stable polar vortex. Figure 2 shows that depletion also extends out through the midlatitudes and into the tropics when heterogeneous chemistry is included in the model. Ozone losses in the tropical lower stratosphere during the depletion era initially came as a surprise (Randel et al., 1999), but in recent years potential contributions from enhanced upwelling as well as chemical drivers have been much discussed (Randel and Thompson, 2011; Solomon, 1999; Solomon et al., 2016a). The patterns of ozone loss in the tropical and subtropical lower stratosphere of the Chem-Dyn-Vol and Vol-Clean runs in Figure 2 show that heterogeneous chemistry plays a substantial role in this region according to WACCM; note that the gas phase case shows ozone decreases near 50 hPa in the deep tropics as well that are likely linked to enhanced upwelling. We elaborate on this in Section 5.

Lobe-shaped patterns of increased depletion in the middle to lower stratosphere extending from the tropics to the subtropics are similar in both the Chem-Dyn-Vol and NoHet40NS (see Figure S3) runs, indicating that much of the low latitude depletion is not produced in situ but rather is the result of horizontal transport of ozone-depleted air from higher latitudes in this model. Looking at the effects of volcanic aerosols on the tropics in the model as a function of pressure and time (Figure S5) also shows both the

dramatic increases in depletion after large-magnitude eruptions and the smaller effects after moderate-sized eruptions.

Comparison with SWOOSH show broad areas of agreement in Figure 2, albeit with differences in detail, with deep depletion in the Antarctic and less depletion in the upper stratosphere. There is a large increase in modeled ozone near and just below the tropopause in the tropics that reaches more than 15% per decade; while part of this may reflect changing tropical dynamics or tropospheric chemistry, SWOOSH is not intended for tropospheric analysis, and some of the trends near the tropopause may be spurious.

In the recovery era shown in Figure 3, SWOOSH generally agrees with the model for all runs in the upper stratosphere, further supporting that the gas-phase chemistry is well represented in models. However, in the lower stratosphere the Chem-Dyn-Vol and Vol-Clean runs suggest positive trends over much of the globe apart from the Arctic that differ from those observed. Large negative trends in SWOOSH near the tropopause in the recovery era in the tropics (see Ball et al., 2018) are not reproduced in these model runs. The basic model pattern (particularly the positive trends in the lower stratosphere seen in all runs including gas-phase) partly reflects dynamical changes in the MERRA fields used to drive SD-WACCM, which are highly uncertain. Previous work found that differences between datasets in the lowermost stratosphere were larger than trends in ozone (Steinbrecht et al. 2017), and tropical trends in

circulation have been shown to vary significantly depending on the reanalysis product used (Abalos et al., 2015). Analysis of the simulations suggests that an accelerating Brewer Dobson circulation in MERRA contributed to the tropical depletion seen directly above the tropopause in the gas-phase run in Figure 2, while the opposite occurred in the recovery era (Figure 3). Increases in ozone at and below the tropopause in this model also trace to tropospheric chemical production and subsequent transport into the lowermost stratosphere. Further analysis of tropospheric ozone trends is beyond the scope of this paper.

The difference between the Chem-Dyn-Vol and Vol-Clean runs is useful in showing where and by how much volcanoes have impeded recovery; this is especially noticeable in the Antarctic and Arctic lower stratosphere but is also significant in the mid latitudes (see also Figures S4 and S6). SWOOSH shows somewhat weaker recovery in the mid-stratosphere (30 to 10 hPa) than the model; however, in all cases the trends here are very small, and natural dynamical variability is likely to be important (Stone et al., 2018).

Figures S6 and S7 show profile trends in more detail for different regions: 90° to 70° for the poles, 60° to 45° for the midlatitudes, 30° to 15° for the subtropics, and 15° to 0° for the tropics. Comparing the difference between starting dates for the depletion era in 1979 versus 1984 (Figure S8) shows that the volcanic influence is sensitive to the timeframe chosen. As the latter start date begins during the influence of El Chichón,

when ozone is already depleted from that eruption, the volcanic impacts over the time period appear smaller, whereas beginning in 1979 before the El Chichón eruption captures that volcano's effect. Removing tropical heterogeneous chemistry shows a slight difference of order 1% locally at the levels nearest the tropopause in the subtropics and tropics in this model.

5 Discussion and Conclusions

We have presented simulations using the WACCM model for both the ozone depletion (1979-1998) and recovery (1999-2014) eras to investigate the relative global impacts of heterogeneous chemistry, stratospheric volcanic aerosol loading, and gas-phase chemistry. We compared model-simulated total column ozone trends against both the SBUV and NIWA-BS datasets, and latitude-vertical ozone trends against the SWOOSH dataset.

As is well known, heterogeneous chemistry dominates ozone depletion not only in the Antarctic but also in the global lower stratosphere and total column; here we quantified the contributions to ozone trends from heterogeneous chemistry using a state-of-the-art chemistry-climate model. Volcanoes are shown to have increased the depth of the depletion and have delayed the recovery (at least to 2014 as evaluated here) according to the best current chemical understanding, underscoring the necessity

of including changes in aerosol content when analyzing recovery trends. Ozone trends in the tropics contributed to the global trends in the model in both the depletion and recovery eras, as shown in Table 1. Mixing between latitudes appears significant within this model, with our results indicating that ozone depleted air is transported from higher latitudes into the subtropics (i.e., compare Figures 2 and S3). Within the tropics themselves, in-situ heterogeneous chemistry has small impacts on ozone as well, especially in the depletion era. All of the WACCM runs use the same underlying specified MERRA dynamics, making the contribution from changing chemistry easy to identify but also limiting the analysis that can be performed on changing dynamics.

Observational data broadly agree with our total column ozone analysis within their respective large uncertainties. Lack of satellite coverage for ozone observations before the 1980s, and limited coverage for much of that decade, makes constraining precise pre-depletion values difficult. The Chem-Dyn-Vol run shows a deeper depletion during the 1991-1997 era of elevated volcanic aerosol from Mt. Pinatubo and Cerro Hudson, but tracks the data well for the rest of the depletion era, and for much of the recovery. SWOOSH latitude-pressure plot comparisons show general agreement with the model runs, but with divergence near the tropopause and where percentage changes are small. Overall, comparison of the data and model after 1999 suggests that recovery trends are dominated by natural variability in the global lower stratosphere, with volcanic eruptions likely playing a role in this variability. Should the current period

of moderate volcanic activity change to a quiescent one similar to that seen between Mt. Pinatubo and 2004, future ozone recovery can be expected to be easier to discern. The differences between our model runs demonstrate the effects due to changes in sulfate aerosols or heterogeneous chemistry schemes, and underscore the importance of accurate representation of sulfate aerosols. Careful observations and analysis will be necessary to discern and attribute significant trends amid the noise of natural variability as the ozone layer evolves during the 21st century.

Acknowledgments and Data

Table 1

Total Column Ozone Trends (DU/Year) for the Depletion and Recovery Eras and Percentage Differences from Chem-Dyn-Vol for 60°N to 60°S

	1979-1998 Trends (95% CI)	%Δ From Chem-Dyn-Vol	1999-2014 Trends (95% CI)	%Δ From Chem-Dyn-Vol
Chem-Dyn-Vol	-0.829 (-1.030, -0.628)	--	0.130 (-0.005, 0.265)	--
Vol-Clean	-0.700 (-0.806, -0.595)	-15.6%	0.197 (0.097, 0.297)	+51.5%
NoHet40NS	-0.790 (-0.952, -0.627)	-4.7%	0.145 (0.097, 0.297)	+11.5%
Gas-phase	-0.292 (-0.416, -0.168)	-64.8%	0.045 (-0.068, 0.158)	-65.4%
SBUV	-0.633 (-0.790, -0.477)	-23.6%	-0.021 (-0.141, 0.098)	-116.2%
NIWA-BS	-0.502 (-0.643, -0.361)	-39.4%	-0.072 (-0.243, 0.098)	-155.4%

Figure 1: Top: Time series of three year running mean of 60°N-60°S total column ozone anomalies with respect to 1998 values from 1979 to 2014 with Gas-phase, Vol-Clean, and Chem-Dyn-Vol runs shown as green, orange, and blue solid lines. SBUV and NIWA-BS total column ozone data are shown by the black line with circles and the purple line with squares, respectively. Grey triangles at the bottom indicate volcanic eruptions, with the larger triangles indicating eruptions of VEI 5 and 6. Bottom: time series of anomalies in global mean total column ozone and their respective linear fits for the depletion era (left), and for the recovery era (right). Fit parameters are given in Table 1.

Figure 2: Contour plots of linear trends during the SWOOSH depletion era (1984-1998) expressed as percent per decade for the (a) Chem-Dyn-Vol (b) Vol-Clean, (c) Gas-phase runs, and (d) SWOOSH dataset. The white line indicates the location of the tropopause in the model.

Figure 3: As in Figure 2, but for the recovery era (1999-2014).

References

Abalos, M., Legras, B., Ploeger, F., & Randel, W. J. (2015). Evaluating the advective Brewer-Dobson circulation in three reanalyses for the period 1979–2012. Journal of Geophysical Research: Atmospheres, 120(15), 7534-7554.

Ball, W. T., Alsing, J., Mortlock, D. J., Staehelin, J., Haigh, J. D., Peter, T., ... & Bourassa, A. (2018). Evidence for a continuous decline in lower stratospheric ozone offsetting ozone layer recovery. Atmospheric Chemistry and Physics, 18(2), 1379-1394.

Bodeker, G. E., Shiona, H., & Eskes, H. (2005). Indicators of Antarctic ozone depletion. *Atmospheric Chemistry and Physics*, *5*(10), 2603-2615.

Chehade, W., Weber, M., & Burrows, J. P. (2014). Total ozone trends and variability during 1979–2012 from merged data sets of various satellites. Atmospheric Chemistry and Physics, 14(13), 7059-7074.

Davis, S. M., Rosenlof, K. H., Hassler, B., Hurst, D. F., Read, W. G., Vömel, H., ... & Damadeo, R. (2016). The Stratospheric Water and Ozone Satellite Homogenized (SWOOSH) database: A long-term database for climate studies. Earth system science data, 8(2), 461.

Douglass, A. R., Strahan, S. E., Oman, L. D., & Stolarski, R. S. (2014). Understanding differences in chemistry climate model projections of stratospheric ozone. Journal of Geophysical Research: Atmospheres, 119(8), 4922-4939.

Farman, J. C., Gardiner, B. G., & Shanklin, J. D. (1985). Large losses of total ozone in Antarctica reveal seasonal ClOx/NOx interaction. Nature, 315(6016), 207.

Garcia, R. R., Smith, A. K., Kinnison, D. E., Cámara, Á. D. L., & Murphy, D. J. (2017). Modification of the gravity wave parameterization in the Whole Atmosphere Community Climate Model: Motivation and results. Journal of the Atmospheric Sciences, 74(1), 275-291.

Hofmann, D. J., & Solomon, S. (1989). Ozone destruction through heterogeneous

   chemistry following the eruption of El Chichon. Journal of Geophysical Research:

   Atmospheres, 94(D4), 5029-5041.

Keeble, J., Brown, H., Abraham, N. L., Harris, N. R., & Pyle, J. A. (2018). On ozone

   trend detection: using coupled chemistry–climate simulations to investigate early

   signs of total column ozone recovery. *Atmospheric Chemistry and Physics*,

   18(10), 7625-7637.

Klobas, E., J., Wilmouth, D. M., Weisenstein, D. K., Anderson, J. G., & Salawitch, R. J.

   (2017). Ozone depletion following future volcanic eruptions. *Geophysical

   Research Letters*, *44*(14), 7490-7499.

Kyrölä, E., Laine, M., Sofieva, V., Tamminen, J., Päivärinta, S. M., Tukiainen, S., ... &

   Thomason, L. (2013). Combined SAGE II–GOMOS ozone profile data set for

   1984–2011 and trend analysis of the vertical distribution of ozone. Atmospheric

   Chemistry and Physics, 13(21), 10645-1065.

Mahieu, E., Chipperfield, M. P., Notholt, J., Reddmann, T., Anderson, J., Bernath, P. F., ... & Franco, B. (2014). Recent Northern Hemisphere stratospheric HCl increase due to atmospheric circulation changes. Nature, 515(7525), 104.

Marsh, D. R., Mills, M. J., Kinnison, D. E., Lamarque, J. F., Calvo, N., & Polvani, L. M. (2013). Climate change from 1850 to 2005 simulated in CESM1 (WACCM). Journal of climate, 26(19), 7372-7391.

McPeters, R. D., Bhartia, P. K., Haffner, D., Labow, G. J., & Flynn, L. (2013). The version 8.6 SBUV ozone data record: An overview. Journal of Geophysical Research: Atmospheres, 118(14), 8032-8039.

Mills, M. J., Schmidt, A., Easter, R., Solomon, S., Kinnison, D. E., Ghan, S. J., ... & Gettelman, A. (2016). Global volcanic aerosol properties derived from emissions, 1990–2014, using CESM1 (WACCM). Journal of Geophysical Research: Atmospheres, 121(5), 2332-2348.

Molina, M. J., & Rowland, F. S. (1974). Stratospheric sink for chlorofluoromethanes: chlorine atom-catalysed destruction of ozone. Nature, 249(5460), 810.

Naik, V., Horowitz, L. W., Daniel Schwarzkopf, M., & Lin, M. (2017). Impact of volcanic aerosols on stratospheric ozone recovery. *Journal of Geophysical Research: Atmospheres*, *122*(17), 9515-9528.

Neely III, R. R., & Schmidt, A. (2016). VolcanEESM: Global volcanic sulphur dioxide (SO2) emissions database from 1850 to present–Version 1.0. Centre for Environmental Data Analysis, 4 February 2016.

Randel, W. J., Stolarski, R. S., Cunnold, D. M., Logan, J. A., Newchurch, M. J., & Zawodny, J. M. (1999). Trends in the vertical distribution of ozone. Science, 285(5434), 1689-1692.

Randel, W. J., & Thompson, A. M. (2011). Interannual variability and trends in tropical ozone derived from SAGE II satellite data and SHADOZ ozonesondes. Journal of Geophysical Research: Atmospheres, 116(D7).

Rinsland, C. P., Mahieu, E., Zander, R., Jones, N. B., Chipperfield, M. P., Goldman, A.,

    ... & Toon, G. C. (2003). Long-term trends of inorganic chlorine from ground-

    based infrared solar spectra: Past increases and evidence for stabilization.

    Journal of Geophysical Research: Atmospheres, 108(D8).

Rodriguez, J. M., Ko, M. K., & Sze, N. D. (1991). Role of heterogeneous conversion of

    N2O5 on sulphate aerosols in global ozone losses. Nature, 352(6331), 134.

Sofieva, V. F., Kyrölä, E., Laine, M., Tamminen, J., Degenstein, D., Bourassa, A., ... &

    Rahpoe, N. (2017). Merged SAGE II, Ozone_cci and OMPS ozone profile

    dataset and evaluation of ozone trends in the stratosphere. Atmospheric

    Chemistry and Physics, 17(20), 12533-12552.

Solomon, S. (1999). Stratospheric ozone depletion: A review of concepts and history.

    Reviews of Geophysics, 37(3), 275-316.

Solomon, S., Daniel, J. S., Neely, R. R., Vernier, J. P., Dutton, E. G., & Thomason, L.

    W. (2011). The persistently variable "background" stratospheric aerosol layer and

    global climate change. Science, 333(6044), 866-870.

Solomon, S., Garcia, R. R., Rowland, F. S., & Wuebbles, D. J. (1986). On the depletion of Antarctic ozone. Nature, 321(6072), 755.

Solomon, S., Kinnison, D. E., Bandoro, J., & Garcia, R. R. (2015). Simulation of polar ozone depletion: An update. Journal of Geophysical Research-Atmospheres, 120(1), 7958–7974. http://doi.org/10.1002/2015JD023365.

Solomon, S., Kinnison, D., Garcia, R. R., Bandoro, J., Mills, M., Wilka, C., ... & Höpfner, M. (2016a). Monsoon circulations and tropical heterogeneous chlorine chemistry in the stratosphere. Geophysical Research Letters, 43(24).

Solomon, S., Ivy, D. J., Kinnison, D., Mills, M. J., Neely, R. R., & Schmidt, A. (2016b). Emergence of healing in the Antarctic ozone layer. Science, aae0061.

Steinbrecht, W., Froidevaux, L., Fuller, R., Wang, R., Anderson, J., Roth, C., ... & Frith, S. (2017). An update on ozone profile trends for the period 2000 to 2016. Atmospheric Chemistry and Physics, 17(17), 10675-10690.

Stone, K. A., Solomon, S., & Kinnison, D. E. (2018). On The Identification of Ozone Recovery. *Geophysical Research Letters*, *45*, 5158–5165. https://doi.org/10.1029/ 2018GL077955

Vernier, J. P., Thomason, L. W., Pommereau, J. P., Bourassa, A., Pelon, J, Garnier, A., ... & Vargas, F. (2011). Major influence of tropical volcanic eruptions on the stratospheric aerosol layer during the last decade. Geophysical Research Letters, 38(12).

Weber, M., Coldewey-Egbers, M., Fioletov, V. E., Frith, S., Wild, J., Burrows, J. P., ... & Loyola, D. (2018). Total ozone trends from 1979 to 2016 derived from five merged observational datasets-the emergence into ozone recovery. Atmospheric Chemistry and Physics Discussions (ACPD), 2017, 1-37.

Wegner, T., Kinnison, D. E., Garcia, R. R., & Solomon, S. (2013). Simulation of polar stratospheric clouds in the specified dynamics version of the whole atmosphere community climate model. Journal of Geophysical Research: Atmospheres, 118(10), 4991-5002.
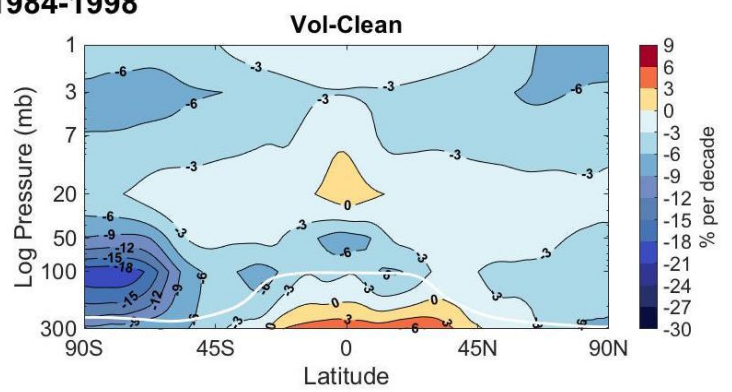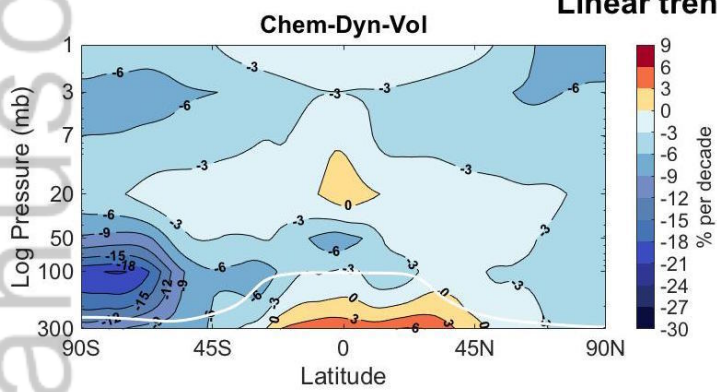
Total Column Ozone Anomaly 1979-2014 from 60°N to 60°S
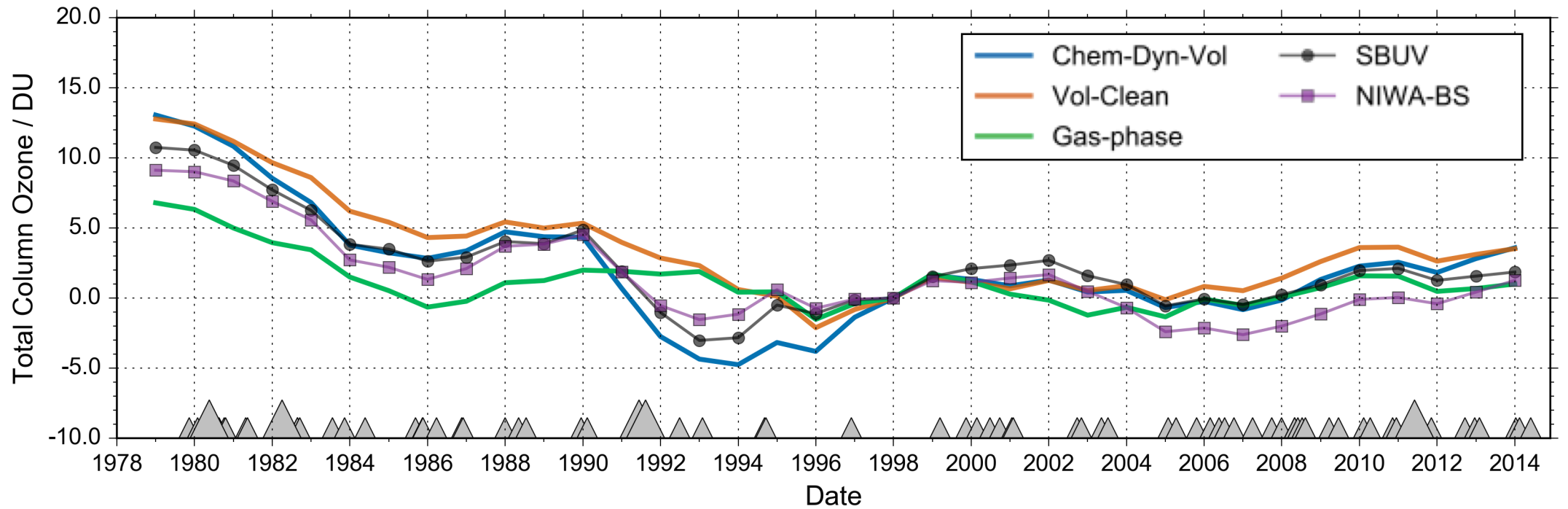
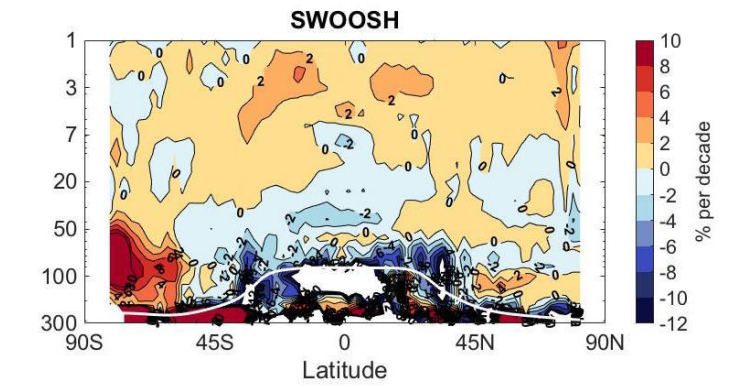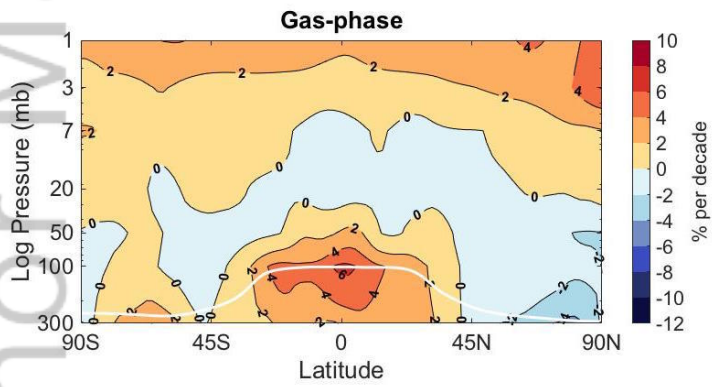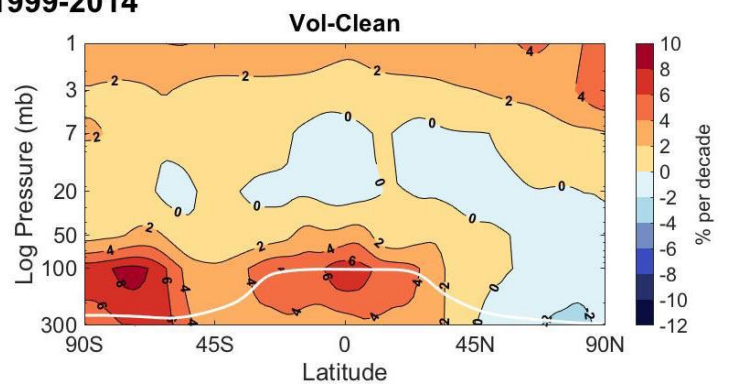Total Column Ozone Anomaly 1979-1998
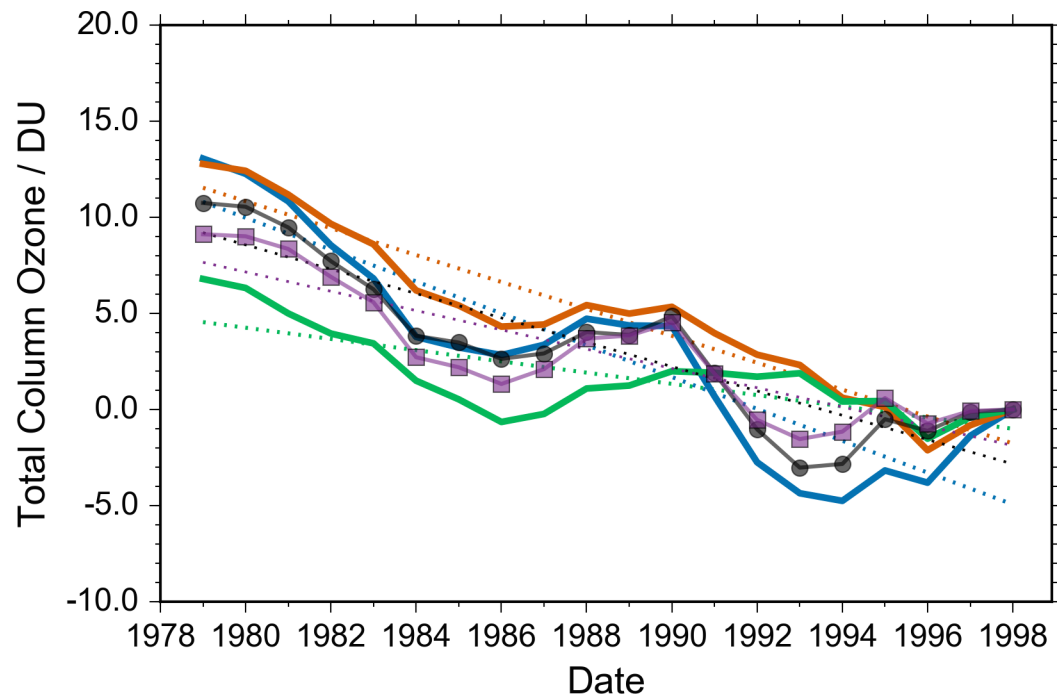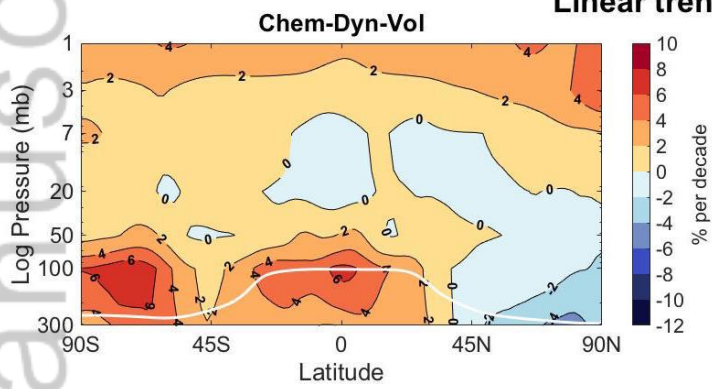
Total Column Ozone Anomaly 1999-2014
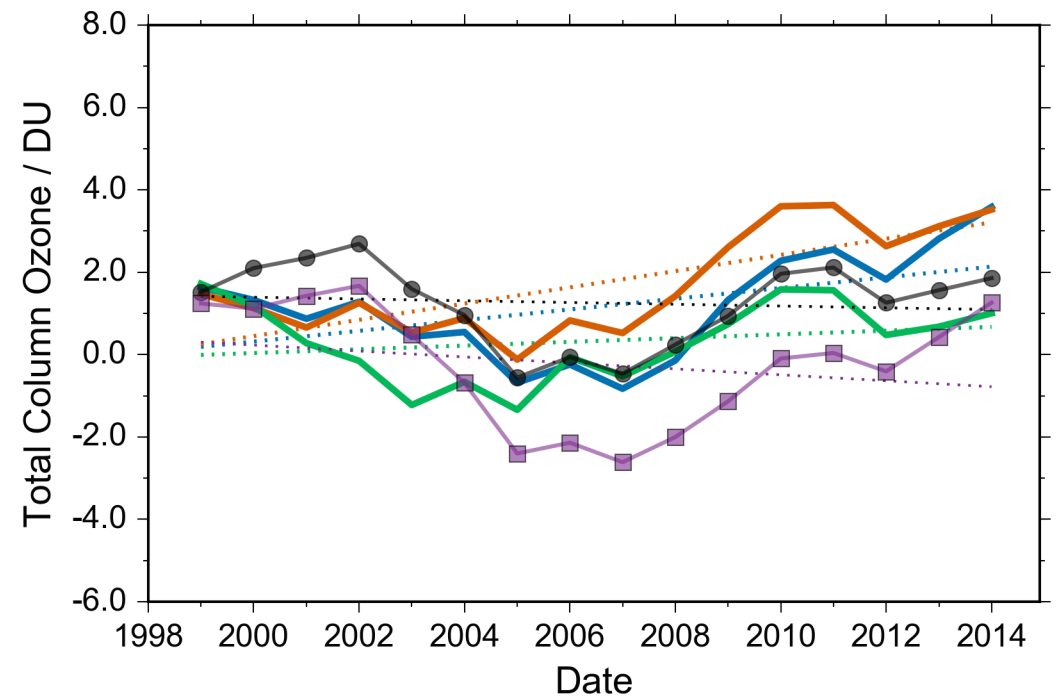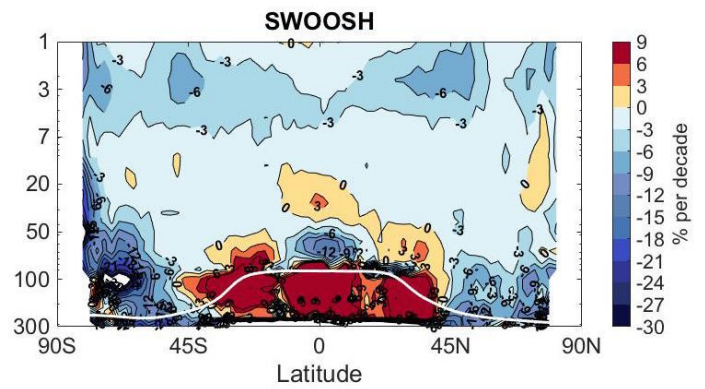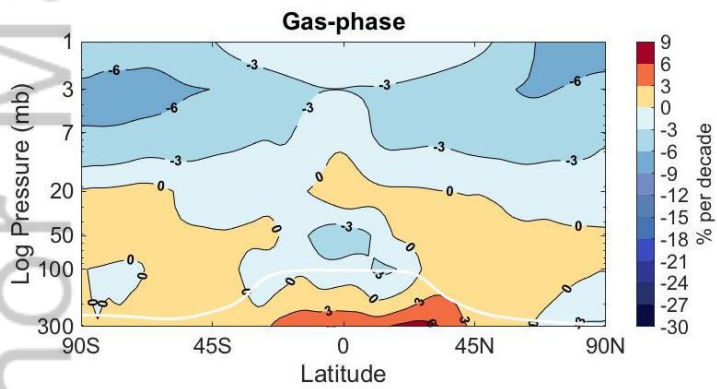
2018GL078596-f02-z-.jpg

2018GL078596-f03-z-.jpg